EVALUATION OF STANDARD OCEAN COLOUR CHLOROPHYLL-a ALGORITHMS IN THE NORTHERN PERSIAN GULF: COMPARISON OF MAGNITUDE AND SEASONALITY

M. Moradi[1] *, K. Kabiri[1]

[1] Iranian National Institute of Oceanography and Atmospheric Science, Tehran, Iran – *moradi_msd@yahoo.com

Commission IV, WG IV/3

KEY WORDS: Remote Sensing, Coastal Waters, Absorption, Phytoplankton, Non-Living Particles

ABSTRACT:

The Persian Gulf is a peripheral sea that is quite turbid and visually complicated. Because of the complicated oceanic and atmospheric optical features of this maritime area, satellite remotely sensed chlorophyll-a (Chl-a, mg m^{-3}) outputs have been used extensively. In this study, the seasonality and magnitude of Level-3 Chl-a time-series products, and daily Level-2 satellite-derived Chl-a concentrations were assessed using corresponding/concurrent in-situ observations gathered during 2008 to 2018. The results revealed that the field observations overestimated satellite-derived Chl-a by 115% in the deeper areas and up to 161% along the Iranian coastal waters. Comparison of inter-annual Chl-a time-series datasets with corresponding in-situ measurements showed that temporal patterns of the satellite-derived Chl-a values are not consistent with field observations. The monthly average of the satellite Chl-a series shows a different seasonal pattern in every region of the study area, and their magnitude over-estimated from 21% to 83% relative to in-situ observations. The absorption coefficients at 488-510 nm are primarily influenced by non-living particles instead of phytoplankton pigments, and no significant correlation are found between in-situ and Chl-a values from OC3/OC4 algorithms. Absorption coefficients spectra of water constituent's shows that the contribution of phytoplankton pigments in particulate absorption coefficients at the blue-green bands are 48%-59%, and the particulate absorptions of water bodies are under the strong influence of non-living particles (40%-52%). Our results suggest that the red-green band-ratios algorithm centred at 675 nm and 555 nm presents more accurate results than OC3/OC4 over the study area.

1. INTRODUCTION

Ocean colour satellite sensors provide important information of chlorophyll-a concentrations and other particle concentrations in surface layer of the seas. Different ocean colour sensors have supported scientists during the past three decades to understand the spatial and temporal patterns of surface chlorophyll contents of the oceans. The Ocean Biology Processing Group (OBPG) of NASA provides an amazing catalogue of ocean colour products extracted from different satellites sensor over the oceans. In general, ocean colour datasets have good agreement with measured chlorophyll in oceanic waters (type I), while their validity decreases in coastal waters where coloured dissolved organic matter (CDOM) and non-algal particles (NAP) are present (Xi et al., 2020). However, ocean colour retrieval algorithms have been applied to optically complex, or Case II, waters where concentrations of phytoplankton do not co-vary with CDOM and non-algal particle loads (Lewis et., 2016). Shallow bottom reflectance, high turbidity, riverine outflows, algae, high CDOM, high concentrations of organic and non-organic particles in coastal areas alter water column properties (Le et al., 2013a). Practically, optical properties of water column are affected by suspended particle matter (SPM, g m^{-3}), non-algal particles (NAP) (a_d, m^{-1}), phytoplankton (a_{ph}, m^{-1}) components, CDOM (a_g, m^{-1}), and particulate absorption (a_p, m^{-1}) (Le et al., 2013). In fact, retrieving precise biogeochemical characteristics and ocean colour parameters in coastal complex water bodies necessitates knowledge of regional optical features (Wang et al., 2019). Therefore, for appropriate use of ocean colour data in optically complex coastal waters, assessment and tweaking of chlorophyll-a (Chl-a) retrieval techniques are crucial.

2. METHODS

2.1 Study area

The biological and chemical properties of the water bodies in the Persian Gulf are significantly impacted by both natural and manmade activity. Large amounts of sediment and nutrients (iron, nitrate, and phosphate) are transferred to the Gulf as a result of these operations, which boosts algal growth and blooms (Al-Yamani and Naqvi, 2019). The Tigris, Euphrates, and Karun rivers, which lie in the northwest, are the main sources of sediment transport to the Gulf. Each year, they release roughly 1.1×108 m^3 of fresh water and 4.8×106 tons of silt (Reynolds, 1993). Additionally, one of the primary elements affecting the growth of phytoplankton in this sea is dust storms coming from nearby nations.

The main factor influencing the seasonal cycles, water circulation patterns, wind stress, and dust deposition in the Persian Gulf is connected to spatial and temporal variability of Chl-a (Al-Najjar et al., 2020). The Persian Gulf has been separated into 5 non-rectangular sub-regions based on bathymetry and circulation patterns in order to research phytoplankton dynamics (Nezlin et al., 2010). (Figure 1).

* Corresponding author

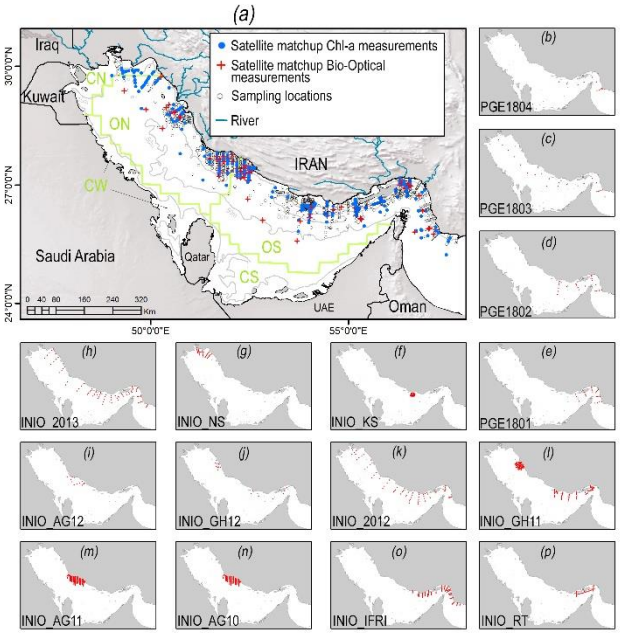

Figure 1. (a) Map of study area and sampling positions. The depth contour lines are displayed as grey lines in meters. The areas described by Nezlin et al. (2010) are shown by green lines and labels. (b) – (p) Various cruise missions' in-situ sample locations.

2.2 Field and Lab measurements

From 2008 to 2018, the Iranian National Institute of Oceanography and Atmospheric Science (INIOAS) collected in-situ samples in the Iranian territorial waters of Persian Gulf. Three identical samples in volume of 1000 mL were taken at each station, at a depth of 0.5 m, using a Niskin container. Before analysis, each sample is vacuum-filtered using a 47 mm Glass Fiber/F filter and stored in the dark at -25°C. 90% acetone was used to extract the chlorophyll pigments overnight, followed by a 10-minute centrifugation. Then, Phytoplankton pigments are used as the source for measuring chlorophyll-a concentrations (mg m^{-3}) using a laboratory flurometer. All analysis were done under low light. On the day of collection, seawater samples' bio-optical characteristics were examined using the techniques Muller et al. specified (2003). SPM (g m^{-1}) samples are measured by filtering through pre-weighed Whatman GF/F filters and combusted in 550°C for 4h, then dried (105°C for 4 h) and weighed. Absorption spectra of non-algal particles (ad(λ), m^{-1}), particulate absorption (ap(λ), m^{-1}), Phytoplankton absorption (aph(λ), m^{-1}), and CDOM absorption (ag(λ), m^{-1}) were measured using a spectrophotometer Shimadzu UV-2600 model and an optional dual detector in the 185 to 1400 nm wavelength range.

2.3 Satellite data

The GlobColour project was started in 2005 by European Space Agency (ESA) to develop long-term and validated dataset of merged Level-3 Ocean Colour products (http://globalcolour.info). The GlobColour project contributes to CMEMS since May 2015 to disseminate data through HERMES web site (http://hermes.acri.fr/). The ESA Ocean Colour Climate Change Initiative (OC-CCI) program presents a time-series of satellite-derived ocean colour dataset by merging data from SeaWiFS, MODIS, and MESIS at the global scale from 1997 to the present (Sathyendranath et al., 2019). With a greater number of observations and an effort to remove inter-sensor biases, the OC-CCI product is mostly comparable to single-sensor products (Belo et al., 2016). Moreover, it uses the POLYMER atmospheric correction algorithm for processing of MERIS data in all versions and to MODIS-Aqua in v5.0 (Sathyendranath et al., 2019), merged products are validated in case II waters using in-situ data (Sathyendranath et al., 2019), and it presents an improved spatio-temporal coverage.

In this study, we use Level-3 mean monthly data products of multi-sensor merged from GlobColour and OC-CCI, and single-sensors of SeaWiFS, MERIS, MODIS, and VIIRS Chl-a datasets from the beginning of each sensor mission to the end of 2018, with spatial resolution of 4 km.

2.4 Statistical methods

Datasets with non-Gaussian distributions and outliers are provided by ocean colour retrieval techniques. Thus, it is not always possible to evaluate the performance of ocean colour algorithms using traditional statistical indicators. More reliable metrics for assessing the ocean colour algorithms are provided by statistical measures based on simple deviations, such as coefficient of determination (R^2), mean absolute percentage error (MAPE), root mean square error (RMSE) in log scale, and the mean difference or bias (δ) (Seegers et al., 2018; Shang et al., 2014; Wang et al., 2019). These markers are described below:

$$MAPE = \frac{1}{n}\sum_{i=1}^{n}\frac{|y_i - x_i|}{x_i} \times 100 \qquad (1)$$

$$\delta = \frac{1}{n}\sum_{i=1}^{n}[Log10(y_i) - Log10(x_i)] \qquad (2)$$

$$\mathrm{RMSE} = \sqrt{\frac{1}{n}\sum_{i=1}^{n}[Log10(y_i) - Log10(x_i)]^2} \qquad (3)$$

Where x and y, respectively, stand for the parameters' in-situ measurements and satellite-derived values, respectively. The statistical measures were computed in Log10 space, and the findings were then translated back into Log10 space for interpretation. After the back-transformation from Log10 space, bias values less than unity indicate a negative bias, with bias values (δ) closest to unity being the least biased (Twardowski and Tonizzo, 2018).

3. RESULTS

3.1 Spatial distribution of Chl-*a*

The spatial comparisons of in-situ and satellite-derived Chl-a are shown in Figure 2. In December 2008, there were significant concentrations of satellite-derived Chl-a readings in the Persian Gulf's eastern region (zone OS) (Figure. 2a). The in-situ Chl-a concentration values are in the range of 8.23-17.86 mg m^{-3}, and the levels of Chl-a >10 mg m^{-3} patches occur together with a developed red tide occurrence. To find the red tide patches, in-situ bio-optical, Chl-a, and MODIS fluorescence data were employed (Moradi and Kabiri, 2012). Since these samples don't reflect the typical seasonal circumstances of the Persian Gulf, in-situ samples taken from red tide regions (Figure 1p) are removed from statistical analysis. Additionally, river plume zone (CW) displayed the greatest mean monthly Chl-a concentrations (>2.0

mg m^{-3}) throughout the year, with summer and early autumn showing the highest values. Chl-a concentrations > 8.5 mg m^{-3} are seen on satellite data products across the northern coastal waters in September 2011 and November 2012, which is consistent with the matching in-situ observations (Figure 2d, h). According to field observations, there were some spots with high Chl-a values (>5.0 mg m-3) in the spring and summer of 2013 and 2014 in the north-western coastal areas (Figure 2i, j). On satellite data products and in-situ datasets in the summer and winter of 2018 (Figure 2m-o), huge regions of Chl-a concentrations > 7.5 mg m^{-3} are seen.

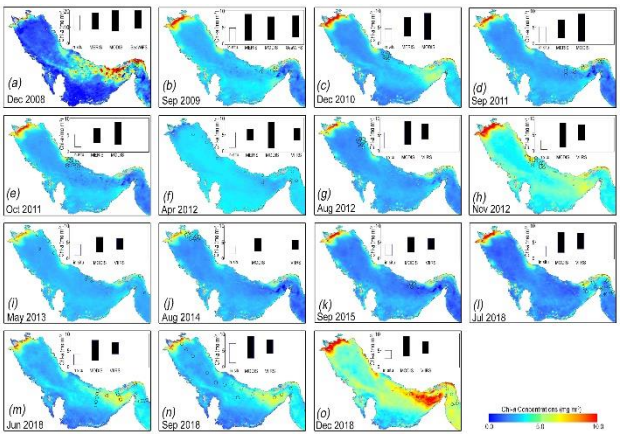

Figure 2. Spatial pattern of in situ Chl-*a* observations. Background values for Chl-a concentrations measured by MODIS during the course of cruise trips are displayed. The range of in-situ measurement values and the range of matched-up satellite-derived Chl-a concentrations are displayed in the column charts on each plate.

The range of in-situ, and satellite-derived Chl-a concentrations reveal that the satellite sensors over-estimated the Chl-*a* concentration values relative to the in-situ observations (Figure 2). In order to describe the accuracy of satellite derived Chl-*a* and demonstrate the similarity and discrepancy of different satellite sensors, in-situ and satellite-derived Chl-*a* data pairs are compared (Figure 3). The results show the consistency of all satellite derived Chl-*a* patterns, but there are large (>25%) differences between them, especially in the river plume zone. The average percentage of errors for all products are more than the 35% threshold value for accuracy indicated by Bailey and Werdell (2006), and Shang et al. (2014). The positive bias (δ) values indicate that satellite-derived Chl-a values are over-estimated relative to in-situ data. The bias (δ) values in coastal (depth<10m) and river plume samples (0.214-0.294) are higher than in deeper zones (0.152-0.195). The MAPE, RMSE and R^2 for entire datasets vary in a range of 115% - 123%, 0.214-0.236 and 0.56-0.59 respectively, that displays good agreement between in-situ observations and satellite-derived Chl-*a*. The poor performance of all satellite-derived Chl-*a* retrieval algorithms (OC3 and OC4) in coastal and river plume regions (MAPE=131-161%, RMSE=0.264-0.326, R2=0.40-0.49) is mainly due to the suspended loads concentrations, and river discharge in shallow waters (Seegers et al., 2018). Moreover, the minimal satellite observation area is around 1 km by 1 km, and often a spatial average in a 3 by 3 box is employed to match the in-situ observation, resulting in a spatial mismatch during validation. Also, the time span of ±6 hours between in-situ observations and satellite overpass and may be too large and introduces some uncertainties in the results.

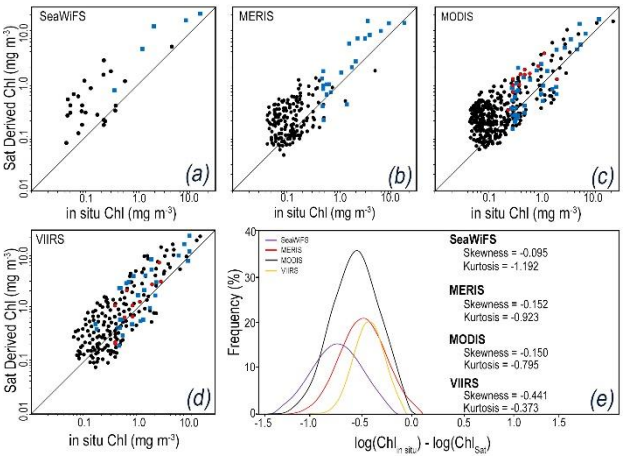

Figure 3. (a) – (d) Statistical comparison of daily satellite-derived Chl-a concentrations in situ and concurrently. Symbols in blue and red colours denote samples from the river plume zone and depths of 10 meters, respectively. (e) Difference between in-situ and satellite-derived Chl-a is distributed log-normally. Statistics are computed using a 95% confidence level.

The log-normal distributions of the differences between in-situ and satellite-derived Chl-a are shown in Figure 3e. The Gaussian distribution of absolute error numbers indicates that RMSE values provide a more accurate assessment of the effectiveness of ocean colour algorithms than MAPE. The RMSE values, however, also highlight how poorly the OC3 and OC4 algorithms perform in coastal and river plume zones. In contrast to the median values of the MERSI, MODIS, and VIIRS curves (MedMERIS = -0.35, MedMODIS = -0.36, and MedViirs = -0.34), the median value of the SeaWiFS curve (MedSeaWifs = -0.67) is significantly smaller. Even if the cause of the algorithmic disparity could not be found, the change in the median values suggests a systemic problem that may be corrected mathematically.

Furthermore, pixel-per-pixel comparisons are performed between satellite sensors (Figure 4). Histogram of difference between pairs of satellite sensors show that that MODIS-SeaWIFS and MERIS-SeaWiFS pairs products estimated the Chl-a concentrations very close to each other (MAPE=24.5-25.6%, RMSE=0.2-0.16, R^2=0.87-0.88). The log-normal distributions of errors between satellite sensor pairs indicate the source of errors are systematic, and we are able to adjust them arithmetically. The MAPE, RMSE, R^2 and bias (δ) values of the other satellite sensor pairs vary in range of 12.03-13.85%, 0.08-0.1, 0.87-0.91, and -0.003-0.027, respectively. Small values of RMSE (averaged 0.12) revealed that the differences between satellite sensors are better than those presented by MAPE values (13.75% - 25.57%). The presented statistical data in Figure 4 reveal that the MODIS, MERIS, and VIIRS have estimated Chl-*a* concentrations very close to each other, and SeaWiFS overestimated the Chl-*a* concentrations more than the others.

3.2 Chl-*a* time-series comparisons

In Figure 5, the corresponding average in-situ data are superimposed over the satellite-derived Chl-a monthly average time series from September 1997 to December 2018. In general,

This contribution has been peer-reviewed. The double-blind peer-review was conducted on the basis of the full paper.
https://doi.org/10.5194/isprs-annals-X-4-W1-2022-531-2023 | © Author(s) 2023. CC BY 4.0 License.

no significant differences between trends and magnitude of merged multi-sensor and single-sensor Chl-a series are observed. This test is run by confidence level of 95%, and hence significance level (p) <0.05 indicates a significant trend. In general, satellite-derived Chl-a series in the areas where field observations are available, show higher values than in-situ measurements. Chl-a levels are increased in winter at deep zones (ON and OS) and in late summer to early fall in shallow zones, according to all Chl-a products from various single satellite and merged sensors (CS and CW). In zone OS, the red tide episode depicted in Figure 2a coincided with the apex of high values of all Chl-a series in December 2008. The Chl-a series also exhibits high values from November to December and low values from July to September in these zones. The low in-situ Chl-a readings in December 2010, December 2011, and December 2012 go counter to this observation. Similar trend is observed in zone ON, except for two in-situ samples in March and November 2012. It is not possible to evaluate the Chl-*a* series in the shallow areas because there are only three corresponding in-situ observations in the river plume zone, and no in-situ observation is available in the southern areas (CS and CW). The Pearson correlation coefficients between monthly Chl-*a* series and corresponding in-situ measurements are in range of 0.62-0.67, 0.59-0.66, 0.58-0.62, 0.57-0.62, and 0.68 for Glob Colour multi-sensor merged, OC-CCI, VIIRS, MODIS, and MERIS, respectively. The merged multi-sensor and single-sensors datasets do not indicate significant differences, and on average the correlation coefficients between in-situ measurements and satellite-derived Chl-*a* are relatively similar. However, the results of the Pearson rank analysis show that there is not a significant association between the in-situ Chl-a levels and the satellite-derived Chl-a series in any of the zones. The findings also demonstrate that none of the satellite data products could be used to estimate the amplitude of the Chl-a series, and the temporal patterns of the series are not highly compatible with field observations.

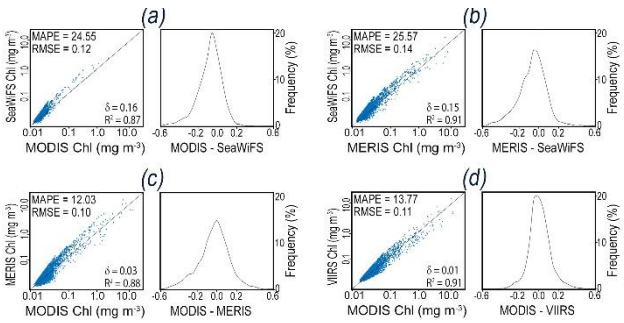

Figure 4. Histogram of difference, and scatter-plot between concentrations of Chl-a from paired of satellite sensors.

The monthly climatology series of satellite-driven Chl-a averages and the corresponding in-situ Chl-a averages in each zone are compared in order to assess the seasonal cycles of Chl-a series over the research region (Figure 6). The seasonal cycles in deeper zones (OS and ON) are characterized by peaks in November-December (in OS: Chl=3.0-3.2 mg m-3; in ON: Chl=2.1-2.6 mg m^{-3}), and a depression in April-Jun (in OS: Chl=1.6-1.9 mg m^{-3}; in ON: Chl=1.4-1.6 mg m^{-3}) (Figure 6a, b). While, seasonal cycles show a peak in August-November in shallow zones (in CS: Chl=2.8-3.1; in CW: Chl=3.0-3.7 mg m^{-3}), the trend of variations are relatively uniform from February to Jun (Chl=1.6-2.6 mg m^{-3}) (Figure 6c, d). Maximum and minimum levels of Chl-a are seen in the river plume zone (CN) in the months of October (Chl=4.3-4.9 mg m-3) and June (Chl=2.7-3.2 mg m-3), respectively (Figure 6e). The greatest values of the shallow and deeper zones are recorded in late summer-early autumn and late winter-early spring, respectively, according to the average trends of monthly climatology readings (Figure 6f). The monthly climatology values show over-estimation of single satellite sensors and multi-sensor merged series in zones OS, ON, and CN (21% - 83% relative to the average of Chl-*a* series). In zone OS, in-situ Chl-a values show a depression in Jun (Chl=0.29 mg m^{-3}), which could not be observed in satellite Chl-*a* series and it is over-estimated by 80% - 86% and 82% by single sensors and multi-sensor merged datasets, respectively. The rate of overestimation of monthly climatology in zone OS decreases in spring and winter. In this zone, the minimum value of Chl-*a* overestimation is observed in March with 15%-36% for single sensors, and 22% for merged datasets. In zone ON, the minimum values of monthly averaged in-situ measurements is observed in May, and the values of over-estimation between monthly climatology of Chl-*a* and corresponding in-situ data vary from 0.62% to 0.85%. In the river plume zone (CN) the monthly climatology values of satellite-derived Chl-a show 0.62%-0.89% overestimation relative to the corresponding in-situ measurements. The greatest and minimum values of overestimation in relation to the corresponding in-situ measurements are displayed in monthly climatology data collected from SeaWiFS and MODIS for zones OS, ON, and CN (when in-situ data are available). In contrast, neither merged multi-sensor datasets nor single-sensor datasets were able to quantify the size of the Chl-a seasonal cycle.

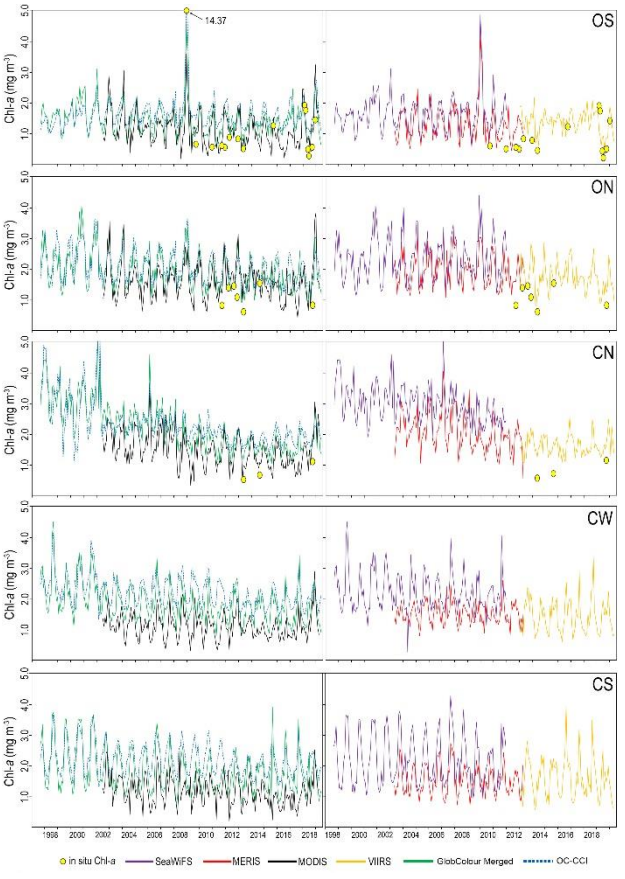

Figure 5. monthly average Chl-a concentrations measured by single and combined satellite sensors over the several Persian Gulf zones in an interannual time series. Corresponding in-situ Chl-a averages for each cruise are represented by filled circles.

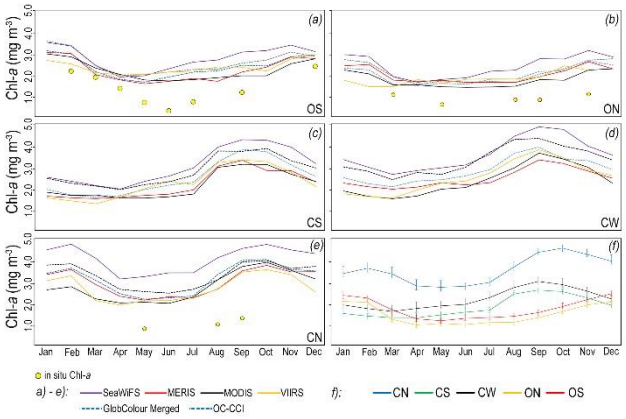

Figure 6. Monthly climatology of single-sensors and multi-sensor merged Chl-a for the different zones of the study area. (a) zone OS, (b) zone ON, (c) zone CS, (d) zone CW, (e) zone CN. (f) averaged values. Filled circles represent the in-situ Chl-a averages over the corresponding zone according to sampling calendar date.

4. DISCUSSION

The findings of this study, as well as earlier ones, demonstrated that the Persian Gulf's Chl-a fluctuation pattern is primarily seasonal and relates to river outflows, water circulation, dust deposition, and climatic regimes. The monthly climatological trends revealed that the deep zones' highest Chl-a concentrations were recorded in late summer and early autumn, whereas the shallow and river plume zones' maximum concentrations were recorded in winter. In all zones, spring was when Chl-a concentrations were at their lowest. A comparison of time series between in-situ Chl-a and satellite-derived Chl-a showed that the OC3 and OC4 algorithms have significant overestimation values (>35%) in the research region. Comparison between temporal patterns and in-situ observations revealed that the magnitude of seasonal cycles could not be quantified accurately. The degree of OC3 and OC4 overestimation relative to in-situ observations was not comparable, and the seasonal patterns of Chl-a averages were noticeably different in time and place, particularly in the winter and in the river plume area. The results indicated that these two empirical algorithms systematically over-estimated the Chl-a concentrations, mainly due to an excess of CDOM and NAP absorptions. In the high turbid case II waters such as Persian Gulf, the OCx algorithms that do not consider the influence of SMP and turbidity generate large errors in Chl-*a* estimation. When SPM values are high (>1 g m^{-3}) in murky environments, the blue-green wavelength band ratio algorithms may overestimate the Chl-a concentrations by up to 20 times for a low concentration of chlorophyll (0.05 mg m^{-3}). An increase of 10 g m^{-3} in the SMP concentration can reduce the chlorophyll fluorescence signals of >50% per unit Chl-*a*. The high concentrations of CDOM at the levels above global mean leads to an over-estimation of satellite-derived Chl-*a* (Lewis et al., 2016). There are also other factors that may explain systematic over-estimation of Chl-*a* from standard OC3/OC4 algorithms, such as uncertainties in atmospheric correction algorithms, high concentrations of suspended sediments, vertical mixings that disturb the stratification of water column, and effects of aeolian dust deposition on the bio-optical properties of the sea water. The study area is subject of strong winds (speed ≅ 16 m s^{-1}) that blow throughout the year. Winds stresses intensify the circulation and induce vertical mixings that disturb the stratification of water column in the Persian Gulf. Therefore, the water bodies in the research area are probably turbid, and high levels of suspended sediments and CDOM values were observed over the whole area. Nezlin et al. (2010) believe that the seasonal cycles of wind regimes and Chl-*a* concentrations in the deeper zones of the Persian Gulf waters do not correlate, and vertical mixing in the water body is not the primary factor regulating phytoplankton growth. They demonstrated that the primary factor affecting Chl-a inter-annual variability is dust deposition. The absorption values in the blue wavelength are often low during dust events or when aerosol concentrations are high in the atmosphere, which causes an overestimation of Chl-a.

The findings of this study revealed a predictable temporal pattern between various satellite Chl-a products in the waters of the Persian Gulf, however significant variations in river plume and shallow zones were found. Chl-a data collected in-situ was utilized to identify the causes of similarities and differences. Due to the small number of in-situ measurements, we must accept that there are certain ambiguities and restrictions in interpreting the study's findings. First, no in-situ observation data were available in the shallow zones, and all in-situ data were acquired from Iranian territorial seas (CN, CW and CS). Second, there may be some ambiguities as a result of the statistical comparisons between satellite and in-situ Chl-a using a small number and threshold of matching pairings. A time span of ± 3 hours, the number of valid pixels, and the variability of pixel values within the given window make up the conventional match-up criteria for in-situ observations and satellite data. In this investigation, a timeframe of ±6 hours were taken into account to get sufficient matchup data pairs. Due to the likelihood that fluctuations in water column characteristics would develop more quickly, this might have a substantial impact on the outcomes. In actuality, the timings of the in-situ data and the satellite flyover time were different, therefore statistical comparisons might introduce some inaccuracies in the outcomes. Future research in the turbid coastal areas is advised to use a tight temporal matching methodology. Third, using conventional blue-green empirical band-ratios algorithms in optically complex water bodies like the Persian Gulf is challenging due to the contribution of CDOM and non-living particles to light absorption in the blue bands and residual errors in the blue bands from imperfect atmospheric correction.

5. CONCLUSION

Using in-situ chlorophyll concentrations and a bio-optical dataset across the northern Persian Gulf, the precision of the conventional OC3 and OC4 Chl-a retrieval methods from the SeaWiFS, MERIS, MODIS, and VIIRS satellite data sets was assessed. Satellites overstated the Chl-a concentrations by up to 161% in coastal areas and by 115% in deeper zones. In the study area's shallow and river plume zones, seasonal and interannual trends of Chl-a products revealed varying amplitude. Chl-a series seasonal and inter-annual volatilities were more uniform in the deeper zones than in the river plume and shallow zones. The amount of overestimation values over the northern portions of the research region were calculated after evaluating the seasonal and inter-annual trends of Chl-a concentrations. The distortion rates of Chl-a seasonality were demonstrated to be considerable. The accuracy of the OC3 and OC4 algorithms at 488–547 nm and 510–555 nm wavelengths, respectively, was assessed using in-situ measurements. The findings showed that CDOM concentrations were generally low and that phytoplankton and non-living particles account for the majority of total water body absorption. Phytoplankton pigment mean absorptions were lower than the sum of NAP and CDOM. Therefore, the Chl-*a* concentrations extracted from OC3 and/or OC4 standard

This contribution has been peer-reviewed. The double-blind peer-review was conducted on the basis of the full paper.
https://doi.org/10.5194/isprs-annals-X-4-W1-2022-531-2023 | © Author(s) 2023. CC BY 4.0 License.

algorithms, and the correspondent seasonal patterns should be used with caution.

ACKNOWLEDGEMENTS

This work has been supported by the Centre for International Scientific Studies & Collaboration (CISSC), ministry of Science Research and Technology, Grant #990203.

REFERENCES

Al-Najjar, M.A., Munday, C., Fink, A., Abdel-Moati, M.A., Hamza, W., Korte, L., Stuut, J.-B., Al-Ansari, I.S., Al-Maslamani, I., de Beer, D., 2020. Nutritive effect of dust on microbial biodiversity and productivity of the Persian Gulf. *Aquatic Ecosystem Health & Management* 23, 122–135.

Al-Yamani, F., Naqvi, S.W.A., 2019. Chemical oceanography of the Arabian Gulf. Deep Sea Research Part II: Topical Studies in *Oceanography* 161, 72–80.

Belo Couto, A., Brotas, V., Mélin, F., Groom, S., & Sathyendranath, S., 2016. Inter-comparison of OC-CCI chlorophyll-a estimates with precursor data sets. *International Journal of Remote Sensing*, 37(18), 4337-4355.

Le, C., Hu, C., English, D., Cannizzaro, J., Chen, Z., Kovach, C., Anastasiou, C.J., Zhao, J., Carder, K.L., 2013. Inherent and apparent optical properties of the complex estuarine waters of Tampa Bay: what controls light? *Estuarine, Coastal and Shelf Science* 117, 54–69.

Lewis, K.M., Mitchell, B.G., Van Dijken, G.L., Arrigo, K.R., 2016. Regional chlorophyll-a algorithms in the Arctic Ocean and their effect on satellite-derived primary production estimates. *Deep Sea Research Part II: Topical Studies in Oceanography* 130, 14–27.

Moradi, M., Kabiri, K., 2012. Red tide detection in the Strait of Hormuz (east of the Persian Gulf) using MODIS fluorescence data. *International Journal of Remote Sensing* 33, 1015–1028.

Mueller, J.L., Bidigare, R.R., Trees, C., Dore, J., Karl, D., Van Heukelem, L., 2003. Biogeochemical and bio-optical measurements and data analysis protocols: *ocean optics protocols for satellite ocean colour sensor validation*. Revision 4, Vol. 2. NASA/TM-2003 21621, 39–64.

Nezlin, N.P., Polikarpov, I.G., Al-Yamani, F.Y., Rao, D.S., Ignatov, A.M., 2010. Satellite monitoring of climatic factors regulating phytoplankton variability in the Persian Gulf. *Journal of Marine Systems* 82, 47–60.

Reynolds, R.M., 1993. Physical oceanography of the Gulf, Strait of Hormuz, and the Gulf of Oman—Results from the Mt Mitchell expedition. *Marine Pollution Bulletin* 27, 35–59.

Sathyendranath, S., Brewin, R. J., Brockmann, C., Brotas, V., Calton, B., Chuprin, A., ... & Donlon, C., 2019. An ocean-colour time series for use in climate studies: the experience of the ocean-colour climate change initiative (OC-CCI). *Sensors*, 19(19), 4285.

Sathyendranath, S., Stuart, V., Platt, T., Bouman, H., Ulloa, O., Maass, H., 2005. *Remote sensing of ocean colour*: Towards algorithms for retrieval of pigment composition.

Seegers, B.N., Stumpf, R.P., Schaeffer, B.A., Loftin, K.A., Werdell, P.J., 2018. Performance metrics for the assessment of satellite data products: an ocean color case study. *Optics express* 26, 7404–7422.

Shang, S.L., Dong, Q., Hu, C.M., Lin, G., Li, Y.H., Shang, S.P., 2014. On the consistency of MODIS chlorophyll-a products in the northern South China Sea. *Biogeosciences* 11, 269.

Twardowski, M., Tonizzo, A., 2018. Ocean color analytical model explicitly dependent on the volume scattering function. *Applied Sciences* 8, 2684.

Wang, Yueqi, Liu, D., Wang, Yujue, Gao, Z., Keesing, J.K., 2019. Evaluation of standard and regional satellite chlorophyll-a algorithms for moderate-resolution imaging spectroradiometer (MODIS) in the Bohai and Yellow Seas, China: a comparison of chlorophyll-a magnitude and seasonality. *International journal of remote sensing* 40, 4980–4995.

Werdell, P.J., Bailey, S.W., Franz, B.A., Harding Jr, L.W., Feldman, G.C., McClain, C.R., 2009. Regional and seasonal variability of chlorophyll-a in Chesapeake Bay as observed by SeaWiFS and MODIS-Aqua. *Remote Sensing of Environment* 113, 1319–1330.

Xi, H., Losa, S.N., Mangin, A., Soppa, M.A., Garnesson, P., Demaria, J., Liu, Y., d'Andon, O.H.F., Bracher, A., 2020. Global retrieval of phytoplankton functional types based on empirical orthogonal functions using CMEMS GlobColour merged products and further extension to OLCI data. *Remote Sensing of Environment* 240, 111704.